Probing the Electronic Stability of Multiply Charged Anions: Sulfonated Pyrene Tri- and Tetraanions

Xue-Bin Wang,[†] Alina P. Sergeeva,[‡] Xiao-Peng Xing,[†] Maria Massaouti,[§]
Tatjana Karpuschkin,[§] Oliver Hampe,[§,||] Alexander I. Boldyrev,*,[‡]
Manfred M. Kappes,*,[§,||] and Lai-Sheng Wang*,[†]

*Department of Physics, Washington State University, 2710 University Drive, Richland,
Washington 99354, Chemical & Materials Sciences Division, Pacific Northwest National
Laboratory, MS K8-88, Richland, Washington 99352, Department of Chemistry and
Biochemistry, Utah State University, Logan, Utah 84322-0300, Institut für Nanotechnologie,
Forschungszentrum Karlsruhe, P.O. Box 3640, D-76021 Karlsruhe, Germany, and Institut für
Physikalische Cheme, Universität Karlsruhe, Kaiserstraße 12, D-76128 Karlsruhe, Germany*

Received May 4, 2009; E-mail: ls.wang@pnl.gov; a.i.boldyrev@usu.edu;
manfred.kappes@chemie.uni-karlsruhe.de

Abstract: The strong intramolecular Coulomb repulsion in multiply charged anions (MCAs) creates a potential barrier that provides dynamic stability to MCAs and allows electronically metastable species to be observed. The 1-hydroxy-3,6,8-pyrene-trisulfonate {$[Py(OH)(SO_3)_3]^{3-}$ or $HPTS^{3-}$} was recently observed as a long-lived metastable MCA with a large negative electron binding energy of -0.66 eV. Here we use Penning trap mass spectrometry to monitor the spontaneous decay of $HPTS^{3-} \rightarrow HPTS^{\bullet 2-} + e^-$ and have determined the half-life of $HPTS^{3-}$ to be 0.1 s. To explore the limit of electronic metastability, we tried to make the related quadruply charged pyrene-1,3,6,8-tetrasulfonate {$[Py(SO_3)_4]^{4-}$}. However, only its decay product, the triply charged radical anion $[Py(SO_3)_4]^{\bullet 3-}$, as well as the triply charged ion-pairs $[Py(SO_3)_4H]^{3-}$ and $[Py(SO_3)_4Na]^{3-}$, was observed, suggesting that the tremendous intramolecular Coulomb repulsion makes the $[Py(SO_3)_4]^{4-}$ anion extremely short-lived. Photoelectron spectroscopy data showed that $[Py(SO_3)_4]^{\bullet 3-}$ is an electronically stable species with electron binding energies of $+0.5$ eV, whereas $[Py(SO_3)_4H]^{3-}$ and $[Py(SO_3)_4Na]^{3-}$ possess electron binding energies of 0.0 and -0.1 eV, respectively. Ab initio calculations confirmed the stability of these triply charged species and further predicted a large negative electron binding energy (-2.78 eV) for $[Py(SO_3)_4]^{4-}$, consistent with its short lifetime.

I. Introduction

Although multiply charged anions (MCAs) are common in solution and solids, they cannot be easily studied in the gas phase,[1-14] because of the strong intramolecular Coulomb repulsion that renders these species unstable against either autodetachment or charge-separation fragmentation outside condensed media. The electrospray ionization technique has made it possible to produce intense beams of MCAs in the gas phase and allowed their first spectroscopic characterization by photoelectron spectroscopy (PES).[15-21] The electron detachment dynamics of MCAs are strongly influenced by the so-called repulsive Coulomb barrier (RCB) originated from the superposition of the long-range Coulomb repulsion between the remaining anion and the outgoing electron and the short-range polarization attraction/chemical binding of this electron. The RCB prevents slow photoelectrons from being emitted from MCAs, giving rise to a cutoff in photoelectron spectra, which has become a

---

[†] Washington State University and PNNL.
[‡] Utah State University.
[§] Forschungszentrum Karlsruhe.
[||] Universität Karlsruhe.

(1) Scheller, M. K.; Compton, R. N.; Cederbaum, L. S. *Science* **1995**, *270*, 1160.
(2) Freeman, G. R.; March, N. H. *J. Phys. Chem.* **1996**, *100*, 4331.
(3) Schauer, S. N.; Williams, P.; Compton, R. N. *Phys. Rev. Lett.* **1990**, *65*, 625.
(4) Boldyrev, A. I.; Gutowski, M.; Simons, J. *Acc. Chem. Res.* **1996**, *29*, 497.
(5) Dreuw, A.; Cederbaum, L. S. *Chem. Rev.* **2002**, *102*, 181.
(6) Weikert, H. G.; Cederbaum, L. S.; Tarantelli, F.; Boldyrev, A. I. *Z. Phys. D* **1991**, *18*, 299.
(7) Scheller, M. K.; Cederbaum, L. S. *J. Chem. Phys.* **1994**, *100*, 8934.
(8) Boldyrev, A. I.; Simons, J. *J. Chem. Phys.* **1993**, *98*, 4745.
(9) Zakrzewski, V. G.; Ortiz, J. V. *J. Chem. Phys.* **1995**, *102*, 294.
(10) Gnaser, H.; Oechsner, H. *Nucl. Instrum. Methods Phys. Res. B* **1993**, *82*, 518.
(11) Middleton, R.; Klein, J. *Nucl. Instrum. Methods Phys. Res. B* **1997**, *123*, 532.
(12) Hettich, R. L.; Compton, R. N.; Rotchie, R. H. *Phys. Rev. Lett.* **1991**, *67*, 1242.

(13) (a) Boldyrev, A. I.; Simons, J. *J. Phys. Chem.* **1994**, *98*, 2298. (b) Simons, J.; Skurski, P.; Barrios, R. *J. Am. Chem. Soc.* **2000**, *122*, 11893.
(14) Blades, A. T.; Kebarle, P. *J. Am. Chem. Soc.* **1994**, *116*, 10761.
(15) Wang, X. B.; Ding, C. F.; Wang, L. S. *Phys. Rev. Lett.* **1998**, *81*, 3351.
(16) Wang, L. S.; Ding, C. F.; Wang, X. B.; Nicholas, J. B. *Phys. Rev. Lett.* **1998**, *81*, 2667.
(17) Wang, X. B.; Wang, L. S. *Nature* **1999**, *400*, 245.
(18) Wang, L. S.; Wang, X. B. *J. Phys. Chem. A* **2000**, *104*, 1978.
(19) Wang, X. B.; Yang, X.; Wang, L. S. *Int. Rev. Phys. Chem.* **2002**, *21*, 473.
(20) Ehrler, O. T.; Weber, J. M.; Furche, F.; Kappes, M. M. *Phys. Rev. Lett.* **2003**, *91*, 113006.
(21) Wang, X. B.; Wang, L. S. *Annu. Rev. Phys. Chem.* **2009**, *60*, 105.

Scheme 1

$R = OH$ (a),

$SO_3^{\bullet}$ (b),

SO_3H (c),

SO_3Na (d)
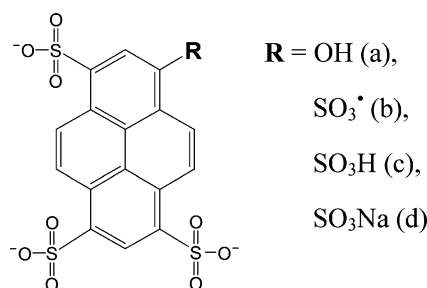
hallmark of PES of MCAs.[15−21] More interestingly, the RCB provides dynamic stability for unstable or metastable MCAs, allowing such exotic species to be observed experimentally.[17,22,23] As a corollary, metastable MCAs store excess electrostatic energies, which are released upon electron detachment. Therefore, metastable MCAs can produce photoelectrons with kinetic energies (KE) *higher* than the detachment laser energy ($h\nu$), resulting in negative electron binding energies (BE) according to Einstein's photoelectric equation: $h\nu = BE + KE$.

The lifetimes of metastable MCAs can be qualitatively estimated[22,24] using the Wentzel−Kramers−Brillouin (WKB) tunneling formalism through a Coulomb potential developed for α-decay in nuclear physics. The lifetimes depend exponentially on the tunneling distance (molecular size) and the magnitude of the negative electron binding energy. Many small MCAs with large negative electron binding energies are too short-lived to allow experimental observation, which is typically on the order of tens of microseconds. The first MCA directly observed to possess a negative electron binding energy was the copper phthalocyanine tetrasulfonate $[CuPc(SO_3)_4]^{4-}$ with a negative electron binding energy of −0.9 eV.[17,23] The relatively small $PtCl_4^{2-}$ dianion was observed to possess a negative electron binding energy of −0.25 eV.[22] The lifetimes of both $[CuPc(SO_3)_4]^{4-}$ and $PtCl_4^{2-}$ have been measured at room temperature in a Fourier-transform ion cyclotron resonance (FT-ICR) mass spectrometer as 275 and 2.5 s, respectivly.[25,26] The long lives of several quadruply charged phthalocyanine systems, $[MPc(SO_3)_4]^{4-}$ (M = Cu, Ni, H$_2$), have been exploited for electronic spectroscopy in the gas phase.[27] Furthermore, femtosecond pump−probe experiments have shown that electron tunneling from excited states is a major relaxation channel in $[H_2Pc(SO_3)_4]^{4-}$.[28] Very recently, a long-lived metastable triply charged anion, 1-hydroxy-3,6,8-pyrene-trisulfonate (HPTS^{3-}) (see Scheme 1a), was observed with a relatively high negative electron binding energy of −0.66 eV and a high RCB of ∼3.3 eV.[29]

In the current work, we explore a general question, that is, how much excess energy can be stored in an MCA of a given

charge state such that its lifetime is still long enough to allow experimental observation and interrogation? The pyrene system (Scheme 1) provides an opportunity to address this question because, by varying the R group, the charge states of the system can be changed while maintaining similar molecular size. We are particularly interested in the R = SO_3^- case to see if the quadruply charged $[Py(SO_3)_4]^{4-}$ species can be observed and how much excess energy it stores. We first measured the lifetime of HPTS^{3-} using Penning trap FT-ICR mass spectrometry and determined its room temperature half-life to be 0.1 s. However, we were not able to observe $[Py(SO_3)_4]^{4-}$, consistent with its large estimated negative electron binding energy of −2.78 eV. We were able to observe its decay product, $[Py(SO_3)_4]^{\bullet 3-}$, and the quadruply charged anions stabilized by H$^+$ and Na$^+$. All these triply charged species, $[Py(SO_3)_4]^{\bullet 3-}$, $[Py(SO_3)_4H]^{3-}$, and $[Py(SO_3)_4Na]^{3-}$, have been shown to be stable by FT-ICR measurements. PES data showed that $[Py(SO_3)_4]^{\bullet 3-}$ possesses a surprisingly high positive electron binding energy of 0.6 eV, whereas the ion-pairs, $[Py(SO_3)_4H]^{3-}$ and $[Py(SO_3)_4Na]^{3-}$, both possess much lower electron binding energies of 0.0 and −0.1 eV, respectively. Ab initio calculations were further carried out to help understand the electronic structures and stability of the pyrene multianions.

II. Experimental and Theoretical Methods

Photoelectron Spectroscopy. The PES experiments were carried out with a low-temperature magnetic-bottle PES apparatus equipped with an electrospray ion source and a cryogenically controlled ion trap. Details of this instrument have been published,[30] and only a brief description is given here. The radical $[Py(SO_3)_4]^{\bullet 3-}$ trianion was observed via electrospray of a 1 mM solution of pyrene-1,3,6,8-tetrasulfonic tetrasodium salt dissolved in a water/ acetonitrile solvent mixture (1/1 volume ratio) that was aimed to produce $[Py(SO_3)_4]^{4-}$, but no trace of the intended quadruply charged anion was observed due to its high instability. It was found that adding acetonitrile, instead of methanol, in the solvent makes the electrospray more stable without the complication of introducing a proton source. The monoprotonated and sodiumated triply charged anions, $[Py(SO_3)_4H]^{3-}$ and $[Py(SO_3)_4Na]^{3-}$, were produced from a water/ methanol solvent mixture (1/3 volume ratio). The $[Py(SO_3)_4]^{\bullet 3-}$ autodetachment product was also observed in this condition and could not be resolved from $[Py(SO_3)_4H]^{3-}$ in the time-of-flight mass spectrum due to their close *m/z* ratios.

Anions from the electrospray source were guided by a radio frequency quadrupole and octopole and then bent 90° into the temperature-controlled ion trap, where they were accumulated and collisionally cooled before being pulsed out into the extraction zone of a time-of-flight mass spectrometer. The ion trap was attached to the cold head of a closed-cycle helium refrigerator to allow ion temperatures to be controlled between 10 and 350 K via collisional cooling with ∼1 mTorr helium background gas containing 20% H$_2$. The ion trap was operated at 70 K in the current experiment. The desired anions were mass selected and decelerated before detachment by a laser beam in the interaction zone of a magnetic-bottle photoelectron analyzer. Two detachment photon energies were used in the current study: 193 nm (6.424 eV) from an ArF excimer laser and 266 nm (4.661 eV) from a Nd:YAG laser. Both lasers were operated at a 20 Hz repetition rate with the ion beam off on alternating laser shots for background subtraction. Photoelectrons were collected at nearly 100% efficiency by the magnetic-bottle and analyzed in a 5.2-m-long electron flight tube. Time-of-flight photoelectron spectra were collected and converted to kinetic energy spectra calibrated with the known spectra of I$^-$ and ClO$_2^-$.

(22) Wang, X. B.; Wang, L. S. *Phys. Rev. Lett.* **1999**, *83*, 3402.
(23) Wang, X. B.; Ferris, K.; Wang, L. S. *J. Phys. Chem. A* **2000**, *104*, 25.
(24) Wang, X. B.; Ding, C. F.; Wang, L. S. *Chem. Phys. Lett.* **1999**, *307*, 391.
(25) Weis, P.; Hampe, O.; Gilb, S.; Kappes, M. M. *Chem. Phys. Lett.* **2000**, *321*, 426.
(26) Arnold, K.; Balaban, T. S.; Blom, M. N.; Ehrler, O. T.; Gilb, S.; Hampe, O.; van Lier, J. E.; Weber, M.; Kappes, M. M. *J. Phys. Chem. A* **2003**, *107*, 794.
(27) Kordel, M.; Schooss, D.; Gilb, S.; Blom, M. N.; Hampe, O.; Kappes, M. M. *J. Phys. Chem. A* **2004**, *108*, 4830.
(28) Ehrler, O. T.; Yang, J.-P.; Sugiharto, A. B.; Unterreiner, A. N.; Kappes, M. M. *J. Chem. Phys.* **2007**, *127*, 184301.
(29) Yang, J.; Xing, X. P.; Wang, X. B.; Wang, L. S.; Sergeeva, A. P.; Boldyrev, A. I. *J. Chem. Phys.* **2008**, *128*, 091102.

(30) Wang, X. B.; Wang, L. S. *Rev. Sci. Instrum.* **2008**, *79*, 073108.

The energy resolution (ΔKE/KE) of the magnetic-bottle electron analyzer was about 2%, i.e., ~20 meV for 1 eV electrons.

Unimolecular Decay and Lifetime Measurements. Lifetime measurements were performed on a FT-ICR mass spectrometer employing a passively shielded 7-T magnet. Gas-phase anions were generated using an electrospray ionization source (Analytica of Branford) with an on-axis sprayer as previously described.[31] The sprayed solutions comprised, respectively, 1-hydroxy-3,6,8-pyrene-trisulfonic acid (for HPTS^{3-}) and tetrasodium pyrene-1,3,6,8-tetrasulfonate hydrate {for [Py(SO$_3$)$_4$]$^{4-}$} (both Sigma-Aldrich, >98% purity) at concentrations of ~10^{-5} mol/L in methanol/water mixtures (3:1). The generated ions were trapped in an ICR cell, the temperature of which can be controlled over a range of 90−400 K at typical base pressures <2 × 10^{-10} mbar. The resolution of the FT-ICR mass spectrometer ($M/\Delta M$) was ~10^5, allowing unequivocal assignments of all relevant anions. For the lifetime studies, the parent MCAs were mass-selected in the ICR cell, and mass spectra were taken after variable time delays of up to 100 s. Decay kinetics was obtained by integrating and normalizing the parent and fragment ion intensities.

Ab Initio Calculations. Theoretical calculations were performed to obtain the optimal structures and vertical detachment energies (VDEs) for comparison with the experimental data. Geometry optimization and vibrational frequency calculations for HTPS^{3-}, [Py(SO$_3$)$_4$]$^{4-}$, [Py(SO$_3$)$_4$]$^{\bullet 3-}$, [Py(SO$_3$)$_4$H]$^{3-}$, and [Py(SO$_3$)$_4$Na]$^{3-}$ were carried out using the hybrid density functional theory (DFT) method known in the literature as B3LYP[32−34] with augmented correlation-consistent polarized double-ζ valence basis sets (aug-cc-pVDZ) for O and Na atoms[35] and correlation-consistent polarized double-ζ valence basis sets (cc-pVDZ) for C, H, and S atoms.[35,36] The VDE for all the species was calculated at the B3LYP/O/aug-cc-pVDZ/H,C,S/cc-pVDZ//B3LYP/O/aug-cc-pVDZ/H,C,S/cc-pVDZ level of theory as the lowest energy transition from the ground state of the optimized M^{n-} species to the state of $M^{(n-1)-}$ at the frozen geometry of M^{n-}. Higher VDEs were obtained using the time-dependent DFT method (TD-B3LYP/O/aug-cc-pVDZ/H,C,S/cc-pVDZ) by adding the vertical excitation energies in $M^{(n-1)-}$ at the optimized geometry of M^{n-} to the first VDE. Natural bond orbital (NBO) analysis was performed at the B3LYP/O/aug-cc-pVDZ/H,C,S/cc-pVDZ//B3LYP/O/aug-cc-pVDZ/H,C,S/cc-pVDZ level of theory to show the natural charge distribution in all the species and how the net charge in the peripheral groups affects the energy of the highest occupied molecular orbital (HOMO) and thus the stability of the MCAs. The B3LYP calculations and NBO analysis were performed using the Gaussian 03 program.[37] Molecular orbital visualization was done using the MOLDEN 3.4 program.[38]

III. Experimental Results

Lifetime Measurements for HPTS^{3-}. The PES spectra of HPTS^{3-} were recently reported, revealing a comparatively large negative electron binding energy of −0.66 eV.[29] During the PES experiment, the HPTS^{3-} anions were stored and cooled in an ion trap for about 50 ms without visible signal loss, suggesting that they are quite long-lived. In the current study, we have directly measured the lifetime of HPTS^{3-} using FT-ICR mass spectrometry. The metastability of HPTS^{3-} was
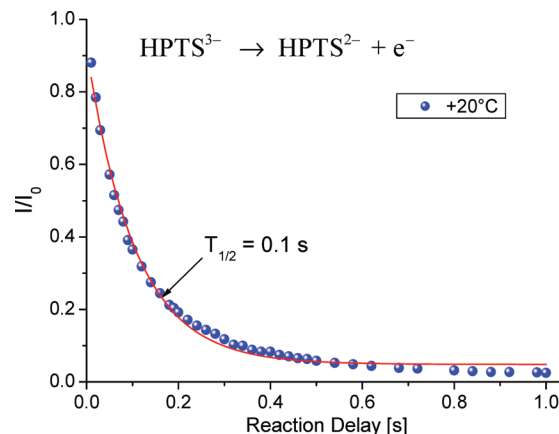

Figure 1. Unimolecular decay of the metastable HPTS^{3-} trianion (via autodetachment of the unbound electron). The half-life is measured to be 0.1 s from the single exponential fit (solid red curve).

immediately confirmed by the appearance of the HPTS$^{\bullet 2-}$ daughter ion in the FT-ICR mass spectra. Figure 1 displays the autodetachment kinetics of HPTS^{3-} at room temperature. An exponential decay was observed, for which a half-life of 0.1 s is deduced from a single-exponential fit. Note that, on the time scale of the decay experiment, the collisional mass loss in the ICR cell was negligible at the UHV pressure. In order to shed some light on the autodetachment mechanism, we have calculated thermionic emission rate constants corresponding to a classical "over-the-barrier" process using statistical unimolecular rate theory as recently outlined.[39,40] Figure S1 (Supporting Information) shows the rate constants obtained as a function of internal energy for three different values of RCB (note the RCB was previously determined to be ~3.3 eV[29]). From these data we conclude that at room temperature (~0.7 eV average internal energy) the detached electron must indeed be *tunneling* through the RCB, because the *classical* thermionic process is orders of magnitude slower than the experimental observation for any conceivable internal energy or barrier height.

Attempt To Observe the [Py(SO$_3$)$_4$]$^{4-}$ Quadruply Charged Anion. We electrosprayed a pyrene-1,3,6,8-tetrasulfonic acid tetrasodium salt solution but did not observe any quadruply charged anion [Py(SO$_3$)$_4$]$^{4-}$, as expected. We were only able to observe triply charged anions (Figure 2), including the auto-detachment product of the tetraanion, [Py(SO$_3$)$_4$]$^{\bullet 3-}$, and two ion-pairs, [Py(SO$_3$)$_4$Na]$^{3-}$ and [Py(SO$_3$)$_4$H]$^{3-}$, in which the parent tetraanion was stabilized by Na$^+$ and H$^+$, respectively. High-resolution FT-ICR mass spectra indicated that the trianions formed depended somewhat on the solvent. [Py(SO$_3$)$_4$]$^{\bullet 3-}$ and [Py(SO$_3$)$_4$Na]$^{3-}$ were generated by electrospray from a pure aqueous solution of the pyrene-1,3,6,8-tetrasulfonic acid tetra-sodium salt. When a water−methanol solution was used, the protonated species, [Py(SO$_3$)$_4$H]$^{3-}$, was also observed, as shown in the inset of Figure 2. The protonated tetraanion was likely formed through ion−molecule reactions with methanol during the electrospray or ion transport processes. An analogous variation of ionic products upon addition of methanol was recently observed from electrospray of amino acids.[41,42] Lifetime measurements showed that all the trianions, [Py(SO$_3$)$_4$]$^{\bullet 3-}$, [Py(SO$_3$)$_4$H]$^{3-}$, and [Py(SO$_3$)$_4$Na]$^{3-}$, displayed no measurable

(31) Blom, M.; Hampe, O.; Gilb, S.; Weis, P.; Kappes, M. M. *J. Chem. Phys.* **2001**, *115*, 3690.
(32) Becke, A. D. *J. Chem. Phys.* **1993**, *98*, 5648.
(33) Vosko, S. H.; Wilk, L.; Nusair, M. *Can. J. Phys* **1980**, *58*, 1200.
(34) Lee, C.; Yang, W.; Parr, R. G. *Phys. Rev. B* **1988**, *37*, 785.
(35) Dunning, T. H., Jr. *J. Chem. Phys.* **1989**, *90*, 1007.
(36) Woon, D. E.; Dunning, T. H., Jr. *J. Chem. Phys.* **1993**, *98*, 1358.
(37) Frisch, M. J.; et al. *Gaussian 03*, Revision C.02; Gaussian, Inc.: Wallingford CT, 2004.
(38) Schaftenaar, G. *MOLDEN3.4*; CAOS/CAMM Center: The Netherlands, 1998.

(39) Concina, B.; Neumaier, M.; Hampe, O.; Kappes, M. M. *J. Chem. Phys.* **2008**, *128*, 134306.
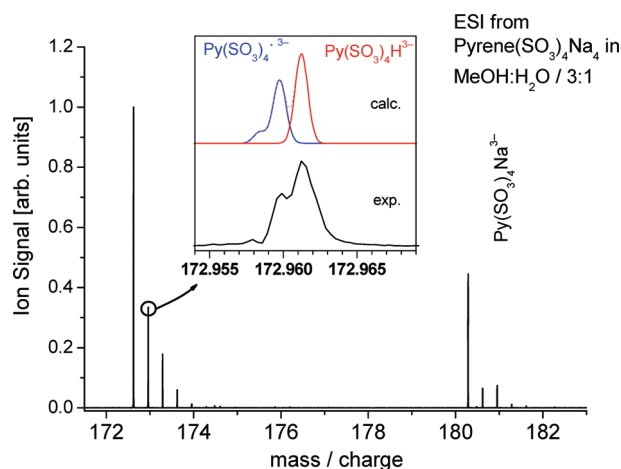(40) Concina, B.; Neumaier, M.; Hampe, O.; Kappes, M. M. *Int. J. Mass Spectrom.* **2006**, *252*, 110.

Figure 2. Negative-ion electrospray FT-ICR mass spectrum showing the region around the isotopomer-resolved triply charged species. The inset shows an enlarged view (around $m/z = 172.96$), revealing contributions from $[Py(SO_3)_4]^{\bullet 3-}$ and $[Py(SO)_4H]^{3-}$ in comparison with simulations.
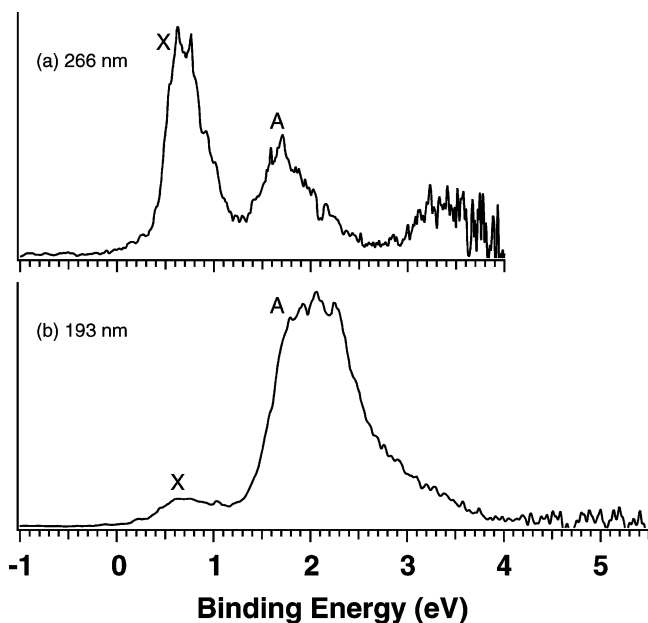

Figure 3. Photoelectron spectra of $[Py(SO_3)_4]^{\bullet 3-}$ at (a) 266 nm (4.661 eV) and (b) 193 nm (6.424 eV).

decays on a time scale of 100 s, suggesting that all these species either are electronically stable or possess half-lives of at least 100 s.

Photoelectron Spectra of $[Py(SO_3)_4]^{\bullet 3-}$. The time-of-flight mass spectrometer in the low-temperature PES apparatus[30] was not sufficient to resolve $[Py(SO_3)_4]^{\bullet 3-}$ and $[Py(SO_3)_4H]^{3-}$. The FT-ICR mass spectrometric results were used to help identify source conditions to distinguish the two trianions. Figure 3 displays the 70 K PES spectra of $[Py(SO_3)_4]^{\bullet 3-}$ at two photon energies obtained by electrospray of a H_2O/CH_3CN solution. The FT-ICR study mentioned above suggested that only $[Py(SO_3)_4]^{\bullet 3-}$ with negligible $[Py(SO_3)_4H]^{3-}$ was produced under this condition. The 193 nm spectrum (Figure 3b) shows a weak, broad feature (X) at low binding energy with a VDE of ~0.6

(41) Tian, Z.; Kass, S. R. *J. Am. Chem. Soc.* **2008**, *130*, 10842.
(42) Tian, Z.; Wang, X. B.; Wang, L. S.; Kass, S. R. *J. Am. Chem. Soc.* **2009**, *131*, 1174.

Table 1. Experimental Adiabatic (ADE) and Vertical (VDE) Detachment Energies and the Estimated Repulsive Coulomb Barriers (RCB) for $[Py(SO_3)_4]^{3-}$, $[Py(SO_3)_4H]^{3-}$, and $[Py(SO_3)_4Na]^{3-}$ [a]

species	ADE (expt)[b]	VDE (expt)[c]	VDE (theor)	RCB[d]
$Py(SO_3)_4^{3-}$	0.50 ± 0.05	0.60 ± 0.05	0.64	3.0
$Py(SO_3)_4H^{3-}$	0.0 ± 0.1	0.0 ± 0.1	0.09(I); −0.01 (II)[e]	3.0
$Py(SO_3)_4Na^{3-}$	-0.1 ± 0.1	-0.1 ± 0.1	0.00(I); −0.10 (II)[e]	3.0
$Py(SO_3)_4^{4-}$			−2.78	
$HTPS^{3-}$(f)	-0.66 ± 0.05	-0.62 ± 0.05	−0.70	3.3

[a] Calculated VDEs are included for comparison. All energies are in eV. [b] The ADE was estimated by drawing a straight line at the leading edge of the 266 nm spectral band at 70 K and then adding the instrumental resolution to the intersection with the binding energy axis. The uncertainty is largely due to the fact that the rising edge is not perfectly smooth. [c] Measured from the maximum of the first band from the 266 nm spectra at 70 K. For the triply charged ion-pairs, the listed VDEs should be regarded as rough estimates due to existence of two isomers and multiple transitions (see Figure 7). [d] Estimated from the 266 nm spectral cutoff compared to the 193 nm spectra (see text). [e] (I) and (II) refer to structures I and II for each species (see Figure 5). [f] Data from ref 29.

eV and a strong band (A) spanning the range from 1.5 to 2.8 eV. At 266 nm, the X feature became dominant, while only the low binding energy part of the A band was observed due to the RCB cutoff. From this cutoff, we estimated a RCB of ~3.0 eV, which is quite close to the previously estimated RCB of 3.3 eV for $HTPS^{3-}$. The weak feature around 3.5 eV in the 266 nm spectrum (Figure 3a) was likely due to detachment of the product dianion $[Py(SO_3)_4]^{\bullet 2-}$ from the same detachment laser pulse. The adiabatic detachment energy (ADE) of $[Py(SO_3)_4]^{\bullet 3-}$ was evaluated from the onset of the 266 nm spectrum by drawing a straight line along the leading edge and adding the instrumental resolution to the intersection with the binding energy axis. We obtained an ADE of 0.5 eV for $[Py(SO_3)_4]^{\bullet 3-}$ (Table 1), which is surprisingly high in comparison to the negative electron binding energy of −0.66 eV for $HTPS^{3-}$, considering their very similar molecular compositions and structures.

Photoelectron Spectra of $[Py(SO_3)_4H]^{3-}$ and $[Py(SO_3)_4Na]^{3-}$. Figure 4a,b shows the spectra of $[Py(SO_3)_4H]^{3-}$ at two photon energies, produced using a water/methanol solution. As shown by the high-resolution FT-ICR study above, a mixture of $[Py(SO_3)_4]^{\bullet 3-}$ and $[Py(SO_3)_4H]^{3-}$ was produced when spraying a water/methanol solution. Thus, the PES spectra in Figure 4a,b should contain contributions from both $[Py(SO_3)_4]^{\bullet 3-}$ and $[Py(SO_3)_4H]^{3-}$ because they could not be separated in the time-of-flight mass spectrometer during the PES experiment. Indeed, the spectral features coming from $[Py(SO_3)_4]^{\bullet 3-}$ can be readily recognized, specifically the X band. The weaker, lower binding energy feature (X′) should come from $[Py(SO_3)_4H]^{3-}$. The higher binding energy features from both species overlap with each other. The threshold of the X′ band yielded an ADE of 0.0 eV for $[Py(SO_3)_4H]^{3-}$ (Table 1), which is considerably less stable than $[Py(SO_3)_4]^{\bullet 3-}$.

The PES spectra of $[Py(SO_3)_4Na]^{3-}$ at 266 and 193 nm are shown in Figure 4c,d. Three broad features (X, A, and B) centered at 0.15, 1.7, and 3.3 eV, respectively, were resolved at 193 nm. The sharp falloff on the high binding energy side of the B band is due to the RCB cutoff effect, allowing the RCB barrier height to be determined as ~3 eV. At 266 nm, some fine structures were observed around the X band region (Figure 4c), which might suggest the existence of conformers or isomers. The A band was cut off due to the RCB. The ADE (−0.1 eV, Table 1) determined from the threshold of the X band for
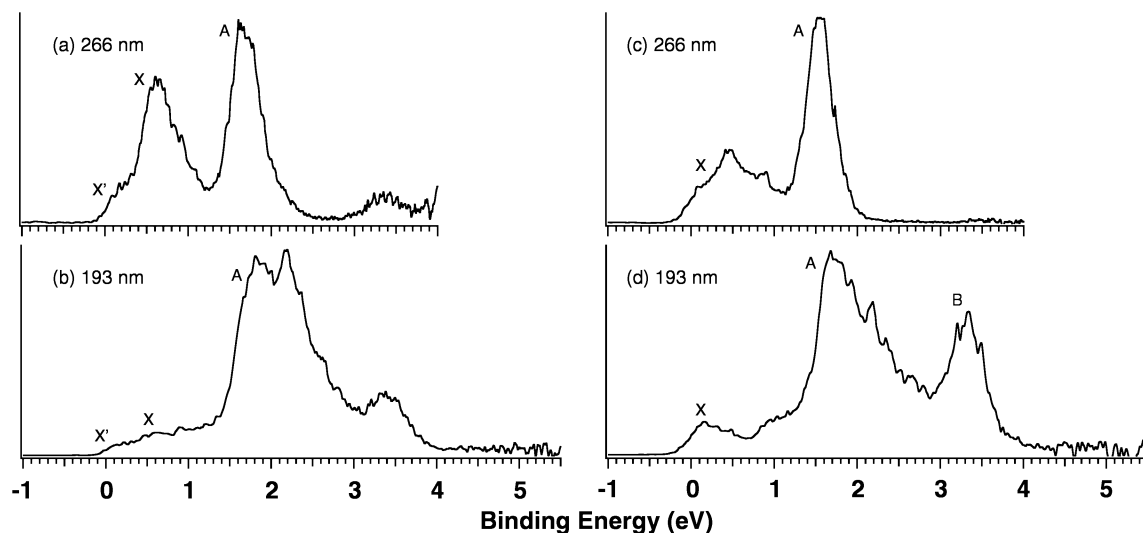
Figure 4. Photoelectron spectra of a mixture of $[Py(SO_3)_4H]^{3-}$ and $[Py(SO_3)_4]^{\bullet 3-}$ at 266 nm (a) and 193 nm (b), and of $[Py(SO_3)_4Na]^{3-}$ at 266 nm (c) and 193 nm (d).
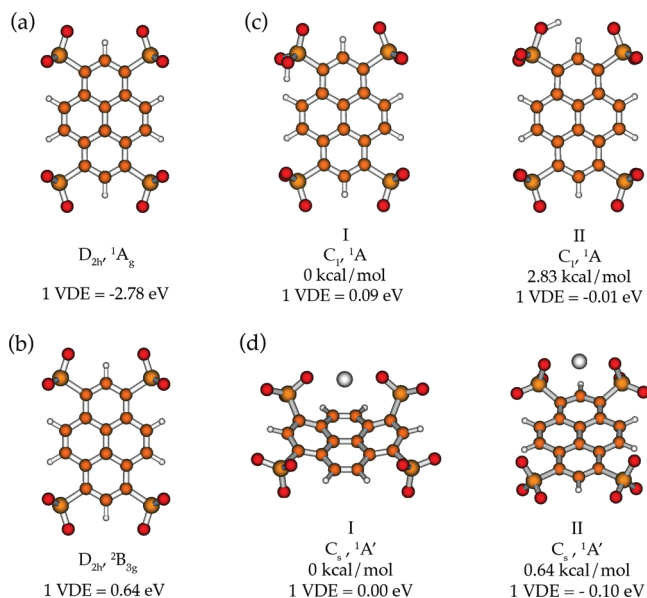

Figure 5. Optimized structures, symmetries, spectroscopic states, and the first VDEs for (a) $[Py(SO_3)_4]^{4-}$, (b) $[Py(SO_3)_4]^{\bullet 3-}$, (c) two low-lying isomers (I and II) of $[Py(SO_3)_4H]^{3-}$, and (d) two low-lying isomers (I and II) of $[Py(SO_3)_4Na]^{3-}$. Relative energies are given at the B3LYP/O/aug-cc-pVDZ/H,C,S/cc-pVDZ level of theory and are corrected for zero-point vibrational energy.

$[Py(SO_3)_4Na]^{3-}$ is slightly negative, suggesting that this trianion is weakly electronically metastable.

IV. Theoretical Results and Discussions

Ab initio calculations were performed to optimize the MCAs' structures, sort out possible isomers, and compute the VDEs to compare with the experimental spectra. Figure 5 displays the optimized structures along with the computed first VDE for each species. The top few molecular orbitals for each species are shown in Figure 6.

$[Py(SO_3)_4]^{4-}$. This quadruply charged anion is closed-shell (^1A_g) with D_{2h} symmetry (Figure 5a). The calculated first VDE lies at -2.78 eV, followed by a transition at -2.09 eV. In fact, the first 20 VDEs were all calculated to be negative. Therefore,
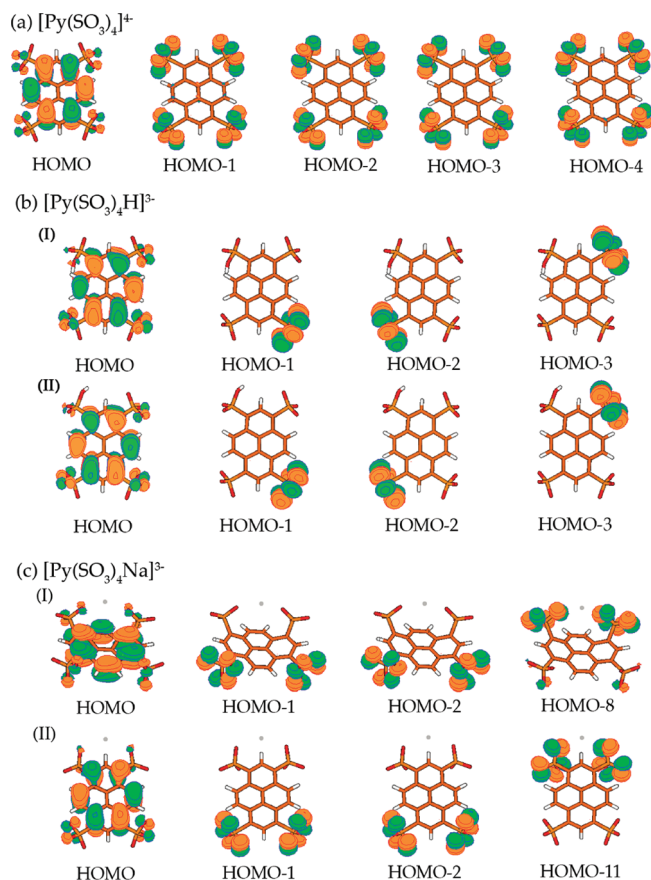

Figure 6. Selected top molecular orbitals for (a) $[Py(SO_3)_4]^{4-}$ (similar molecular orbitals were obtained for $[Py(SO_3)_4]^{\bullet 3-}$), (b) two low-lying isomers (I and II) of $[Py(SO_3)_4H]^{3-}$, and (c) two low-lying isomers (I and II) of $[Py(SO_3)_4Na]^{3-}$.

$[Py(SO_3)_4]^{4-}$ was predicted to be a very unstable species, in agreement with the experimental observations or lack thereof. As in the case of HTPS^{3-},[29] the HOMO of $[Py(SO_3)_4]^{4-}$ is also found to be on the center part of the molecule, consisting of an antibonding π orbital associated with the pyrene rings (Figure 6a). The center part of the molecule experiences the strongest Coulomb repulsion from the peripheral negatively charged SO$_3^-$
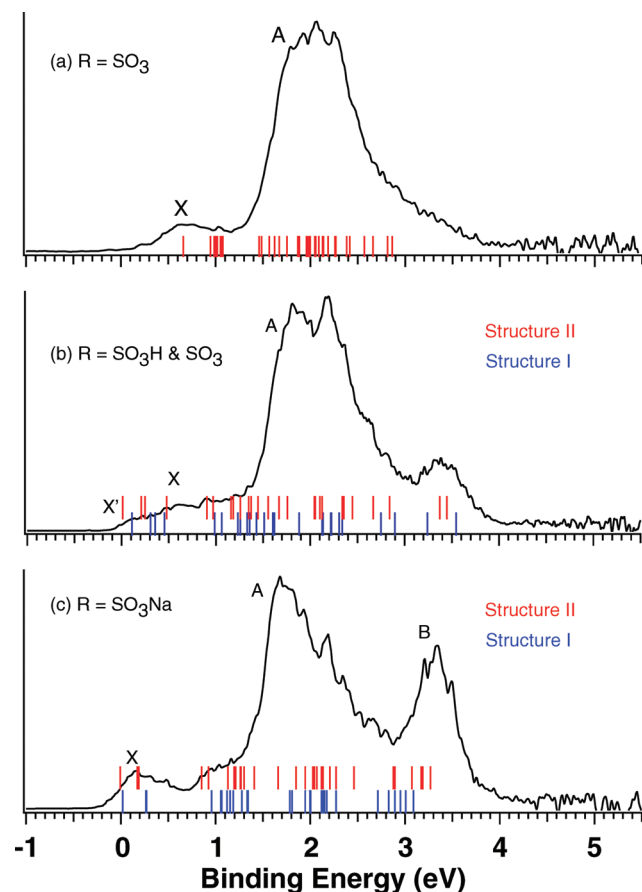
Figure 7. Comparison of the 193 nm photoelectron spectra of $[Py(SO_3)_3R]^{3-}$ [R = SO_3 (a), SO_3H and SO_3 (b), and SO_3Na (c)] with calculated VDEs (solid vertical bars). In (b) and (c), the bottom bars (blue) represent calculated VDEs for structure I, whereas the top bars (red) represent calcucated VDEs for structure II (see Figure 5). In (b), only the calculated VDEs for R = SO_3H are shown; those for R = SO_3 can be seen in (a).

groups, resulting in the large negative electron binding energies for this tetraanion. This is similar to $CuPc(SO_3)_4^{4-}$, the first MCA to be observed with a large negative electron binding energy.[17,23] The HOMO of $CuPc(SO_3)_4^{4-}$ was also found to be on the center part of the molecule because of the enormous Coulomb repulsions from the peripheral negative charges. However, $CuPc(SO_3)_4^{4-}$ is bigger than $[Py(SO_3)_4]^{4-}$, resulting in a comparatively smaller negative electron binding energy (−0.9 eV) and a much longer lifetime.

$[Py(SO_3)_4]^{•3-}$. $[Py(SO_3)_4]^{•3-}$ is a radical anion with an unpaired electron ($^2B_{3g}$ ground electronic state) and D_{2h} symmetry (Figure 5b). The first VDE was calculated to be 0.64 eV, in excellent agreement with the experimental data of 0.6 eV (Table 1 and Figure 3). We computed the VDEs up to ∼2.9 eV and compared them with the experimental PES spectra in Figure 7a. Because of the large size of the molecule, the density of electronic state is quite high. The computed VDEs (displayed as solid bars) are in good agreement with the observed PE spectra. The molecular orbitals of the radical trianion are nearly the same as for the quadruply charged parent anion (Figure 6a).

$[Py(SO_3)_4H]^{3-}$. Two low-lying isomers were found for the $[Py(SO_3)_4H]^{3-}$ anion, both of C_1 symmetry and ^1A ground state (Figure 5c). The proton is attached to one of four equivalent SO_3^- groups, thus neutralizing one charge, which significantly reduced the intramolecular Coulomb repulsion and stabilized

the trianion. Isomer II, which is only 2.83 kcal/mol higher in energy, can be obtained from isomer I by rotating the −SO_3H group by 120° along the C−S bond. We computed the VDEs up to ∼3.5 eV for both isomers. They compare well with the PES spectra, as shown in Figure 7b. Since our PES experiment was taken at 70 K, the contributions from isomer II were expected to be minor. The calculated first VDE (0.09 eV for isomer I) is in excellent accord with the X′ feature in Figure 4a, lending further support to the assignment of this feature to $[Py(SO_3)_4H]^{3-}$. It is also worth noting that the calculated VDEs show no transitions around 0.6 eV from the protonated trianions (Figure 7b), consistent with the assignment of the main X peak in Figure 4a to the radical trianion $[Py(SO_3)_4]^{•3-}$.

Figure 6b displays the top four HOMOs for the two isomers of the protonated trianions. The HOMO in each case is similar to the parent tetraanion, coming from the pyrene-based anti-bonding π orbital.

$[Py(SO_3)_4Na]^{3-}$. Two nearly degenerate isomers were identified for this species, both with C_s symmetry and a $^1A′$ closed-shell ground state (Figure 5d). Isomer II was found to be higher in energy than isomer I by only 0.64 kcal/mol. The calculated first VDE was 0.00 eV for isomer I and −0.10 eV for isomer II, which both agree well with the PES spectra in Figure 4c, suggesting the presence of isomer II experimentally. VDEs were calculated up to 3.2 eV, as compared with the PES spectra in Figure 7c. The top three molecular orbitals for both isomers of $[Py(SO_3)_4Na]^{3-}$ are shown in Figure 6c. The HOMO of both isomers is again the pyrene-based antibonding π orbitals, similar to the parent tetraanion, followed by the orbitals from oxygen lone-pairs on the two peripheral sulfonate groups that are not attached with the Na^+ cation. It is interesting to note that the oxygen lone-pair orbitals derived from the sulfonate groups directly interacting with the Na^+ cation are significantly stabilized, becoming HOMO−8 for isomer I and HOMO−11 for isomer II (Figure 6c).

Factors Controlling Electronic Stability of MCAs. Despite their having the same total charges as well as similar molecular structures, compositions, and HOMOs, the electron binding ability of the four triply charged anions is found to vary over a range of 1.2 eV, from a significantly negative value of −0.66 eV for $HTPS^{3-} \rightarrow -0.1$ eV for $[Py(SO_3)_4Na]^{3-} \rightarrow 0.0$ eV for $[Py(SO_3)_4H]^{3-} \rightarrow +0.5$ eV for $[Py(SO_3)_4]^{•3-}$. For each triply charged anion, the detachment product corresponds to the respective dianion and a free electron. Thus, the electron binding ability or detachment energy is defined as the energy difference between the ground state of the initial triply charged anion and such final detachment product.

It appears that the electronic stability of this series of trianions is very sensitive to the peripheral groups. The OH group in $HTPS^{3-}$ is relatively compact and close to the pyrene ring. Consequently, any negative charge located on its oxygen atom is expected to have a more significant effect on the HOMO, which is centered on the pyrene rings. According to our NBO analysis, each of the three SO_3 groups in $HTPS^{3-}$ contributes a charge of ∼−0.75|e|, whereas the OH group carries a charge of −0.28|e|. In comparison, in $[Py(SO_3)_4H]^{3-}$ each of the three SO_3 groups carries a charge of −0.73|e|, while the fourth protonated sulfonate group is effectively charge neutral due to the screening of the proton. Therefore, a simple electrostatic argument would predict that $HTPS^{3-}$ should be much less stable than $[Py(SO_3)_4H]^{3-}$, consistent with experimental observations.

Why is the radical trianion $[Py(SO_3)_4]^{•3-}$ so much more stable? The net charge on each of the four SO_3 groups in

$[Py(SO_3)_4]^{•3-}$ is $-0.67|e|$, giving rise to a total charge carried by the peripheral groups of $-2.68|e|$, the highest among the trianions. Yet, the electron binding energy of $[Py(SO_3)_4]^{•3-}$ is $+0.5$ eV. This noticeable conflict may be reconciled by considering the radical nature of the $[Py(SO_3)_4]^{•3-}$ species in comparison to the closed-shell molecules of both $HTPS^{3-}$ and $[Py(SO_3)_4H]^{3-}$. The HOMO of the radical trianion is singly occupied, and therefore the Coulomb repulsion is smaller than for the doubly occupied HOMO in the closed-shell trianions, enhancing the electron binding energy. In addition, the extra charges in $[Py(SO_3)_4]^{•3-}$ are completely delocalized among the four peripheral $-SO_3$ groups, thus enhancing the electron binding ability via delocalization, as suggested recently.[43] Alternatively, the radical trianion, $[Py(SO_3)_4]^{•3-}$, may be formally viewed as a zwitterion with a positive hole on the pyrene rings and four peripheral $-SO_3^-$ groups. The positive hole is expected to provide a major stabilizing effect to the remaining electron in the singly occupied molecular orbital, thus enhancing the electronic stability of the radical trianion relative to the closed-shell trianions.

The measured electron binding energy and half-life of -0.66 eV/0.1 s for $HTPS^{3-}$, along with those reported previously for $PtCl_4^{2-}$ (-0.25 eV/2.5 s)[25] and $[CuPc(SO_3)_4]^{4-}$ (-0.9 eV/~275 s),[26] provide a series of benchmarks to predict electronic metastability in doubly, triply, and quadruply charged anions. Given the comparatively long lifetimes of these MCAs, it is conceivable that even higher negative binding energies can be observed in suitably designed doubly, triply, or quadruply charged anions.

V. Conclusions

We report a combined study on the electronic metastability and lifetimes of a series of triply charged anions consisting of a central pyrene scaffold and peripheral sulfonate groups as charge carriers. Autodetachment of $HTPS^{3-}$ to $HTPS^{•2-} + e^-$ was measured in a FT-ICR cell and was used to measure a half-

life of 0.1 s for this metastable trianion, which carries 0.66 eV excess energy. The quadruply charged $[Py(SO_3)_4]^{4-}$ anion, estimated to possess a -2.78 eV negative electron binding energy, was shown to be too unstable to be observed experimentally. Instead, its autodetachment product, $[Py(SO_3)_4]^{•3-}$, as well as ion-pairs stabilized by H^+ and Na^+ were observed and studied both experimentally and computationally. Photoelectron spectroscopy study showed that the $[Py(SO_3)_4]^{•3-}$ trianion is very stable, with an electron binding energy of 0.5 eV, whereas $[Py(SO_3)_4H]^{3-}$ and $[Py(SO_3)_4Na]^{3-}$ are less stable, with electron binding energies of 0.0 and -0.1 eV, respectively.

Supporting Information Available: Unimolecular rate constants calculated for electron loss from metastable $HPTS^{3-}$ ions as a function of internal energies by assuming an over-the-barrier mechanism (i.e., thermionic emission process), and complete ref 37. This material is available free of charge via the Internet at http://pubs.acs.org.

JA903615G

(43) Tian, Z.; Chan, B.; Sullivan, M. B.; Radom, L.; Kass, S. R. *Proc. Natl. Acad. Sci. U.S.A.* **2008**, *105*, 7647.